Low-Power Organic LED Fabricated by a Novel Solution-Based Process for Photoplethysmography Sensing

Seyedfakhreddin Nabavi, *Member, IEEE*, Hossein Anabestani, and Sharmistha Bhadra, *Member, IEEE*

***Abstract*— Power consumption level of electronic devices has always been considered as an important factor for a wide range of applications. In this study, a novel fabrication step, namely, predrying, applicable to solution-based fabrication processes is proposed to minimize the overall power consumption of organic light-emitting diodes (OLEDs). The predry step allows the solution to dwell on the substrate for a certain short time before the spin coater is turned on. It is experimentally shown that the predrying step for OLEDs with the hole transfer layer (HTL) of poly(3,4-ethylenedioxythiophene):poly(styrene sulfonate) (PEDOT:PSS) can reduce the ohmic loss by a factor of 2.41, in addition to reducing the turn-on voltage by 0.9 V and increasing the luminance 1.3 times at 15 V in comparison to the fabricated OLED without predrying step. To further minimize the power consumption of OLEDs, it is proposed to replace PEDOT:PSS with copper(I) thiocyanate (CuSCN) as HTL, which can be deposited by a solution fabrication process including the predrying step. A comparison among the fabricated OLEDs with the predried HTLs made of CuSCN and PEDOT:PSS indicates that the generated luminance increases by a factor of 4.28 from 2.8 to 12 kcd/m^2 for an identical voltage of 11 V. Due to the superior performance of the proposed OLED based on the predried HTL of CuSCN, its behavior as a light source for photoplethysmography (PPG) sensing systems is surveyed. In this article, the PPG sensor is implemented in the form of a flexible-hybrid sensor system, in which the fabricated OLED and a commercial photodiode are housed on a flexible substrate. Results confirm that the implemented flexible-hybrid PPG sensor operating in reflectance mode can acquire high-quality PPG signals with relatively low power consumption and accurately estimate heart rate (HR). The competency of the proposed OLED as a low-power solution for PPG sensor technology is highlighted by comparing its performance with the state of the art.**

***Index Terms*— Flexible hybrid sensor, low power, organic light-emitting diode (OLED), photoplethysmography (PPG) sensing, predying, solution-based fabrication.**

I. Introduction

TO DATE, significant efforts have been undertaken to develop electronic devices with low and near zero power consumption. Light-emitting diodes (LEDs) with low-power, long operational lifetime, and highly embeddable characteristic have proven to be a viable solution for minimizing power consumption in a wide range of illuminating and sensing applications [1]. For example, a matrix of red–green–blue LEDs can be used to create display systems with low power consumption [2], leading to the production of low-weight screen panels. The applicability of LEDs in visible light technology has been extensively reported in the literature [3]. It is worth mentioning that the versatility of LEDs is not only limited to display and communication areas, in medicine, but they also play a crucial role for both diagnosis and treatment. Indeed, LEDs are the principal functional block utilized in photoplethysmography (PPG) sensing systems [4]. In this context, an LED emits light at a specific wavelength onto the skin, and the light reflected/transmitted from the skin is measured by a photodetector. The photodetector current provides vital information about heart rate (HR), blood oxygen saturation, and so on [5], [6].

LED operates on the basis of the electroluminescence (EL) effect. The wavelength (or color) of the light emitted by LEDs depends on the bandgaps of the employed semiconductors. Inorganic LEDs based on II I–V semiconductors, such as GaN and InGaN, led to the development and commercialization of highly efficient and stable LEDs [7]. With the emerging technology of organic electronics that can be used to manufacture eco-friendly flexible devices, solution-based manufacturing of LEDs has attracted significant attention [8], [9]. This has been accepted as a feasible approach to minimize the manufacturing costs of LED, which is highly required for mass production. In this regard, inorganic LED materials are being replaced by organic ones to build new type of light sources called organic LEDs (OLEDs). OLEDs contain an organic emission layer (EML), which offers the unique characteristics of high photoluminescence efficiency, solution processability, and wavelength tunability [10], [11].

The capabilities of OLEDs have continuously improved since their invention in 1987 [12]. The first group of OLEDs used organic fluorescent materials that could only achieve a maximum internal quantum efficiency of 25% [13]. Later, it is shown that the use of phosphorescent materials can improve the light emission efficiency by more than 90% as the emission can be obtained from both singlet and triplet states [14]. Fig. 1 shows the typical structure of a phosphorescent OLED. As can be clearly seen, OLED is a multilayers device with a transparent conductive anode, a hole transport layer

Manuscript received 21 January 2023; revised 15 February 2023; accepted 7 March 2023. Date of publication 20 March 2023; date of current version 25 April 2023. This work was supported in part by the Natural Sciences and Research Council of Canada, MEDTEQ; and in part by the Industrial Partners: iMD Research and Object Research Systems. *(Corresponding author: Seyedfakhreddin Nabavi.)*

This work involved human subjects or animals in its research. Approval of all ethical and experimental procedures and protocols was granted by the Review Board McGill University under Application No. A04-M21-19B.

Seyedfakhreddin Nabavi was with the Department of Electrical and Computer Engineering, McGill University, Montreal, QC H3A 0E9, Canada (e-mail: seyed.nabavi@mcgill.ca).

Hossein Anabestani and Sharmistha Bhadra are with the Department of Electrical and Computer Engineering, McGill University, Montreal, QC H3A 0E9, Canada.

Digital Object Identifier 10.1109/JFLEX.2023.3259384

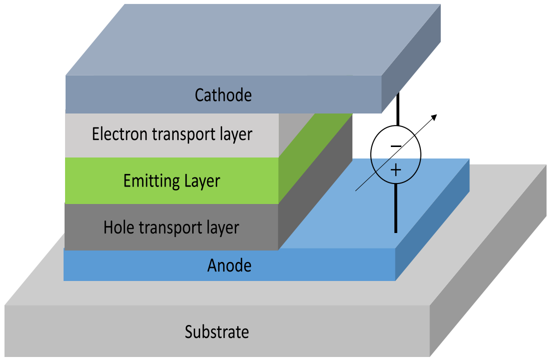

Fig. 1. Typical structural diagram of phosphorescent OLED.

(HTL), an EML, an electron transfer layer (ETL), and a metal cathode. Hence, improving the performance of OLEDs through modifying their material layers is an important objective of many researchers.

A well-known transparent conductive material for the anode of OLEDs is indium tin oxide (ITO). The efficiency of OLEDs is greatly influenced by the work function and surface morphology of ITO [15]. Yahya and Fadavieslam [16], for example, showed that the surface treatment of ITO with argon plasma can improve the efficiency of OLED in terms of turn-on voltage and intensity. Several HTLs, specially the transition metal oxides such as molybdenum oxide (MoO_x), have been employed for their advantageous energy-level alignments [17]. However, MoO_x is deposited by sputtering or electron-beam evaporation. This is less appealing for OLEDs, where a solution-based fabrication method is highly preferred [18], [19]. In contrast, poly(3,4-ethylenedioxythiophene):poly(styrene sulfonate) (PEDOT:PSS) has been widely used as an HTL in the structural layer of many OLEDs by the fact that it can be deposited by spin coating method. Lithium fluoride (LiF) has been effectively implemented as an ETL in many OLED architectures [20]. In this regard, the work function of metal cathode electrodes, e.g., aluminum (Al), is reduced due to the high work function of LiF, resulting in electron transfer [21]. The successful implementation of such a material architecture to fabricate OLEDs operating at different wavelengths, e.g., green and red [22], [23], has already been demonstrated in many studies.

In this study, we are motivated to propose a low-power OLED as a light source for PPG sensors. It is worth mentioning that various approaches are used in the literature to improve the competence of PPG sensors through their analog front-end circuits, such as the multifeedbacks and an additional reference photodiode channel to compensate for dc drifts [24] and a small form factor low-noise integrated circuit with digital microprocessor [25]. In contrast, the focus here is on improving the performance of OLEDs that can be integrated into PPG sensing systems. Hence, a new fabrication process, namely, predrying, applicable to the conventional OLED structure (glass/ITO/PEDOT:PSS/emitter layer/LiF/Al), is proposed to minimize the overall power consumption of OLED. In this fabrication method, a certain delay time is incorporated into the spin coating step to allow the HTL to dwell on the ITO-coated glass. It is experimentally shown that such this simple but effective method can increase the performance of the OLED with PEDOT:PSS as HTL in terms of luminance when compared to a prototype fabricated without a predrying step. Nevertheless, in order to further minimize the power consumption of OLED in addition to increasing its luminance and reducing the turn-on voltage, copper (I) thiocyanate (CuSCN) as the HTL of OLED is employed. This newly used material can be processed in a solution form under ambient conditions, and thus, the HTL can be formed by the spin coating technique comprising the predry step. This means that it does not affect the complexity of OLED manufacturing. A comparison between the performance of OLEDs fabricated based on CuSCN and PEDOT:PSS shows that luminance can be improved, while the turn-on voltage reduces. Due to this significant improvement in attributes of OLED, the OLED based on the predried HTL of CuSCN can be used to build a wearable PPG sensing system, in which low power consumption is highly required.

The rest of this article is organized as follows. The proposed fabrication processes for OLEDs are described in Section II. Section III presents the experimental results along with some additional discussions. The applicability of the proposed OLED as a light source in the form of a flexible-hybrid PPG sensor is shown in Section IV. Eventually, Section V concludes this work.

II. Material Preparation and Fabrication Process

In this study, two types of green wavelength OLEDs were fabricated. The schematics and energy band diagrams of these two types of OLEDs are shown in Fig. 2. As can be seen in Fig. 2, both OLEDs were fabricated on an ITO-coated glass substrate. In the first group of OLEDs, PEDOT:PSS purchased from Ossila is used as HTL, while in the second group of OLEDs, CuSCN is used as HTL. To fabricate CuSCN by a relatively simple solution-based process, 30 g of CuSCN from Sigma Aldrich was dissolved in a 30-mL diethyl sulfide (DES) from Sigma Aldrich and stirred overnight. For the EMLs, a mixture of poly(9,9-di-n-octylfluorenyl-2,7-diyl):poly(9,9-dioctylfluorene-alt-benzothiadiazole) (PFO:F8BT) with a 19:1 ratio is processed in toluene with the total concentration of 10 mg/mL. Then, LiF and Al are used to prepare the ETL and metal cathode electrode, respectively.

According to the energy band diagrams of OLEDs based on the HTLs of PEDOT:PSS and CuSCN, which will be referred to as $OLED_{PS}$ and $OLED_{CN}$, respectively, later in this article, the lowest unoccupied molecular orbital (LUMO) of CuSCN perfectly matches the LUMO of the employed EML. As a result, with CuSCN, holes layer can be more efficiently injected into the EML compared to the PEDOT:PSS HTL layer.

The steps of the solution-based fabrication process used in this study are shown in Fig. 3. As shown in Fig. 3, in the first step, the ITO-patterned glass substrate purchased from Ossila was treated with an oxygen plasma at 90% power for 10 min

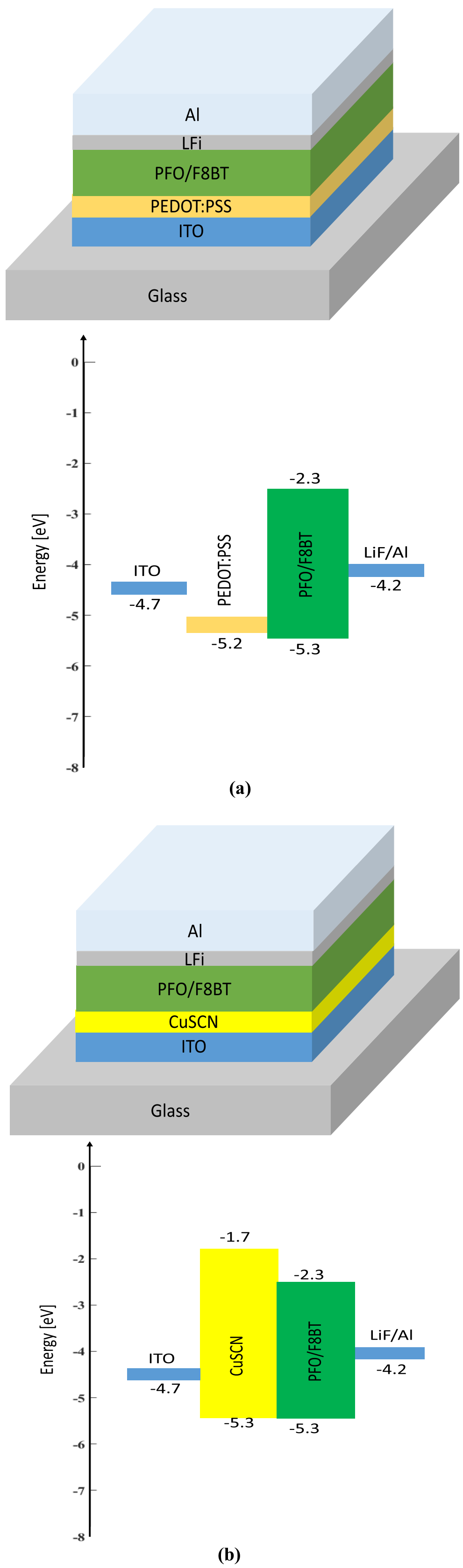

Fig. 2. Structures and energy band diagrams of OLEDs with HTLs. (a) PEDOT:PSS (OLEDPS). (b) CuSCN (OLEDCN).

to improve the hydrophilic properties of the substrate. Then, about 30 nm of HTL (either PEDOT:PSS or CuSCN) was deposited on the substrate using the spin coating technique.

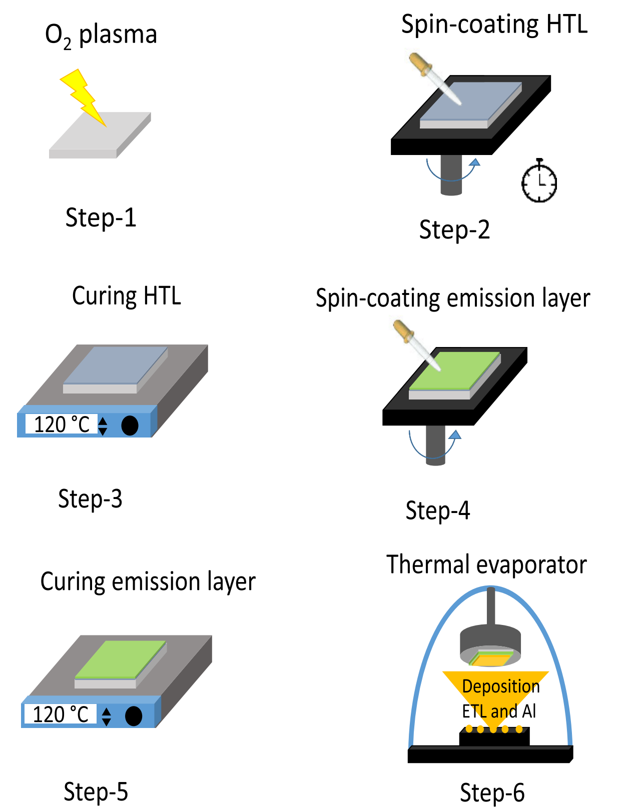

Fig. 3. Employed solution-based fabrication process to fabricate OLEDs.

In this step, the predrying method was used. This means that the solution is placed on the surface of the substrate, and 35 s later, the spin coater is switched on (for without predrying method, the spin coater was turned on right away). After the coating was completed, the device was cured at 120 °C for 10 min. In the next step, the blended solution of the EML was deposited using the spin coating technique in a nitrogen glove box and cured for 10 min at 120 °C. Then, the sample was transferred to a thermal evaporator and 10 nm of the ETL (LiF) and 100 nm of the metal electrode (Al) were deposited at a pressure of about 1×10^{-6} mtorr. To make the OLEDs functional in normal oxygen-containing environment, they were encapsulated with a UV-cured epoxy and cover glasses purchased from Ossila at a power of 0.1 mW/cm^2 for 6 min. In the next section, the effects of predrying step as well as employing CuSCN as the HTL on the performance of the OLED prototypes will be demonstrated.

III. Experimental Results and Discussion

To ensure that the data reported in this section are consistent and statistically valid, each measurement was repeated five times for three different devices and the average of these measurements was plotted. In addition, it should be noted that the maximum deviation observed for each device in the single measurement was about 5%.

To demonstrate the effect of the proposed predrying step on the performance of OLEDs, two OLEDs were fabricated with

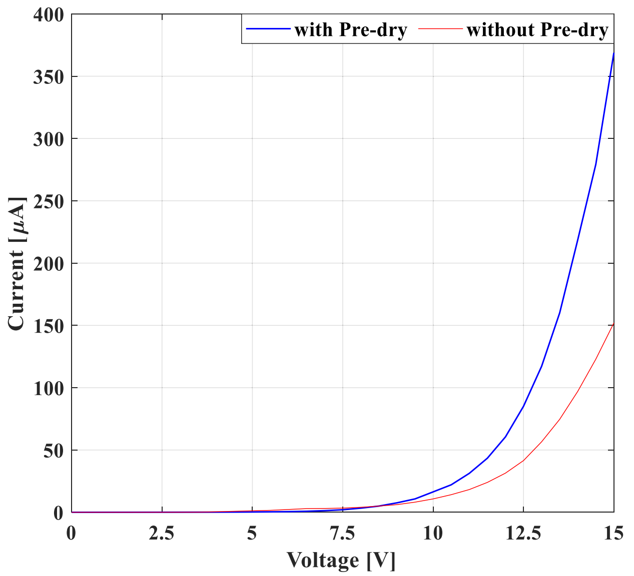

Fig. 4. Measured I–V characteristics of OLED prototypes based on PEDOT:PSS layer fabricated with and without predrying step.

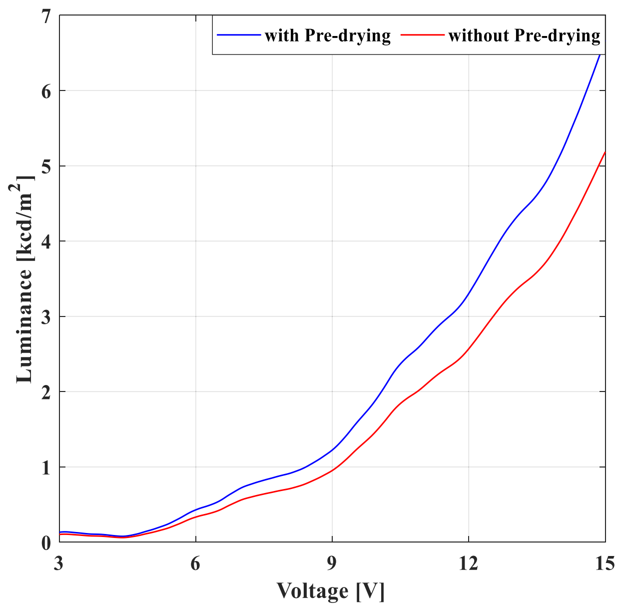

Fig. 6. Measured luminance–voltage characteristics of OLED prototypes based on the PEDOT:PSS layer fabricated with and without predrying step.

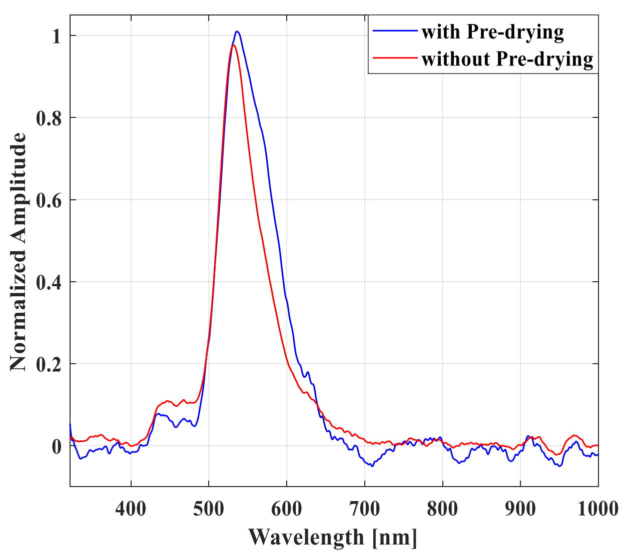

Fig. 5. Measured emission spectra of OLED prototypes based on the PEDOT:PSS layer fabricated with and without predrying step.

the HLT of PEDOT:PSS, one with and one without predrying, using the fabrication process described in Section II.

As first step, the current–voltage (I–V) characteristics of these two OLEDs were measured using a source meter manufactured by Keithley (model 2450). These measured I–V curves are shown in Fig. 4. It is clear that the predrying step leads to a minimization of the ohmic loss of OLED. In this regard, at the same input voltage of 15 V, the current flowing through the OLED prototype fabricated with the predrying step is 368 μA, while the prototype fabricated without the predrying technique can pass a current of 152 μA. This means that the predrying approach can improve the I–V characteristics by a factor of 2.41 (at voltage = 15 V) compared to the prototype fabricated without the predrying step.

The effects of the predrying method on the emission spectrum of the OLEDs are shown in Fig. 5. In this context, the emission intensities of the two fabricated OLEDs (i.e., with and without the predrying step) were measured using a spectrometer manufactured by Ossila when an identical voltage of 15 V was applied to both OLEDs. It can be seen that the peak intensities for both OLEDs are almost a wavelength of 532 nm. However, the predrying step results in a slight broadening of the bandwidth of the emission spectrum.

The OLED's ability to generate sufficient light at low input voltage is a criterion for its performance evaluation. Fig. 6 shows the measured luminance of two OLED prototypes. In this work, the luminance is measured indirectly using the output current of a commercially available photodetector from Vishay (model BPW21R), whose peak sensitivity is at green wavelength. As shown in Fig. 6, the predrying method leads to an increase in luminance by a factor of 1.3 compared to the luminance–voltage curve of the fabricated OLED without predrying at the identical input voltage of 15 V. In addition, predrying can result in a lower turn-on voltage. For example, here, the voltage that leads to a luminance of 1 kcd/m^2 is considered the turn-on voltage, which means that the predried OLED is turned on with a voltage of 8.1 V, while its counterpart is turned on with 9-V input voltage.

To this end, we demonstrated that the use of the proposed predrying method in our solution-based fabrication process can improve the efficiency of OLED_{PS} in terms of ohmic loss, turn on voltage, and luminance without undesirable effects on the emission spectrum. Here, using the same experimental setup described for the characterization of OLED_{PS}, the applicability of CuSCN as HTL for OLED is evaluated in addition to the predrying effect. Fig. 7 shows the I–V relationship for two OLEDs with the HTL of CuSCN fabricated with and without predrying step. It can be observed that the predrying step leads

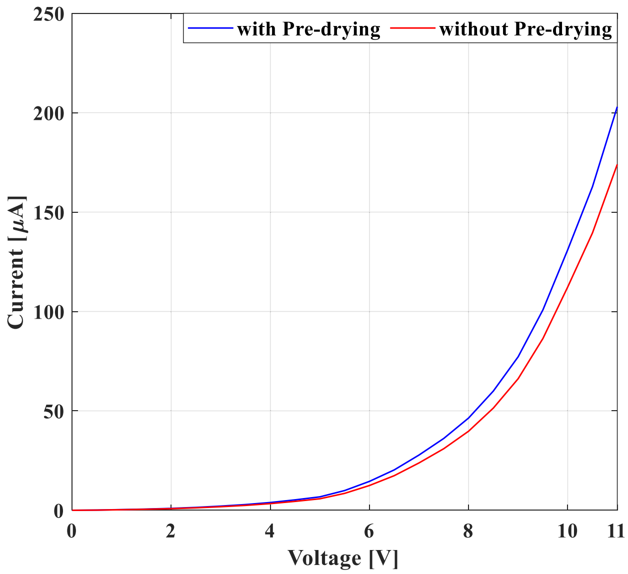

Fig. 7. Measured I–V characteristics of OLED prototypes based on CuSCN layer fabricated with and without predrying step.

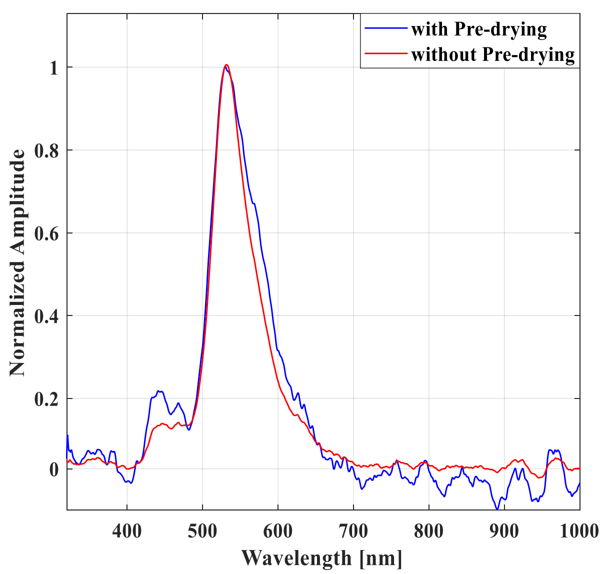

Fig. 8. Measured emission spectra of OLED prototypes based on the CuSCN layer fabricated with and without predrying step.

to a reduction of the ohmic loss compared to the I–V curve of the fabricated OLED without predrying method. At the same input voltage of 11 V, a current of 202 μA flowed, while this was 174 μA for the OLED prototype without predrying. This confirms that predrying can improve the efficiency of OLED_{CN} in terms of ohmic loss by a factor of 1.16 at 11 V.

The measured emission spectra of OLEDs fabricated based on the HTL of CuSCN are depicted in Fig. 8. It is obvious that the use of CuSCN does not affect the peak emission wavelength of OLED compared to the emission spectra of OLED_{PS}, since the maximum emission intensity for both OLED groups is observed at the same wavelength of 532 nm. It is worth noting that, similar to OLED_{PS}, the predrying step causes a slight broadening of the bandwidth.

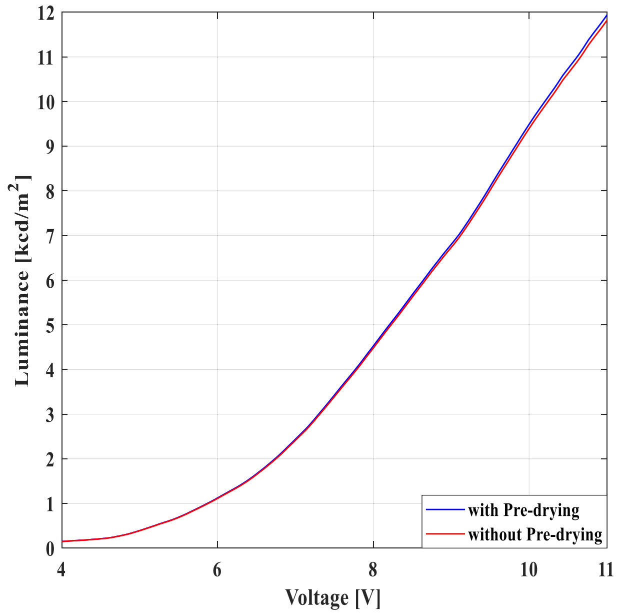

Fig. 9. Measured luminance of OLED prototypes based on the CuSCN layer fabricated with and without predrying step.

The measured luminance of the OLED_{CN} prototypes as a function of voltage is shown in Fig. 9. In Fig. 9, the input voltage was swept from 4 to 11 V and the luminance was estimated based on the photodetector current. From Fig. 9, it can be seen that the predrying method can slightly improve the luminance by only 30 cd/m^2 when the input voltage is 11 V. Furthermore, the turning on of the OLEDs (i.e., voltage of 5.9 V when luminance of 1 kcd/m^2 is produced) remains without change for both fabricated OLEDs. It can be concluded that the predrying method improves OLED performance in terms of luminosity when CuSCN is used; however, the improvement is not considerable for such a nonpolymer-based material.

It is well established that the morphology of films of polymeric materials, which ultimately determines their efficiency, is highly dependent on the method by which they are deposited and their solvent is vaporized. The importance of the vaporization of solvent and its contribution to the crystallinity and roughness of films made from polymeric materials has been discussed in detail in [26] and [27]. In [28], it is reported that solvent vaporization helps to enhance the hole charge carrier mobility and thin-film crystallinity of polymer-based HTL and ETL. Therefore, it can be inferred that the proposed predrying technique that helps to vaporize solvent of the HTL will not only improve the performance of OLED with an HTL made of PEDOT:PSS, but all polymer-based HTL can benefit from this fabrication method. This fabrication step can be of great importance to the OLED field because most organic materials are in the form of polymers. As a result, the proposed fabrication method can lead to the fabrication of highly efficient full-organic LEDs. Full-organic LEDs are advantageous since they can be fabricated at low cost with roll-to-roll printing process as polymeric materials can be formulated easily in the form of ink for printing technologies [29].

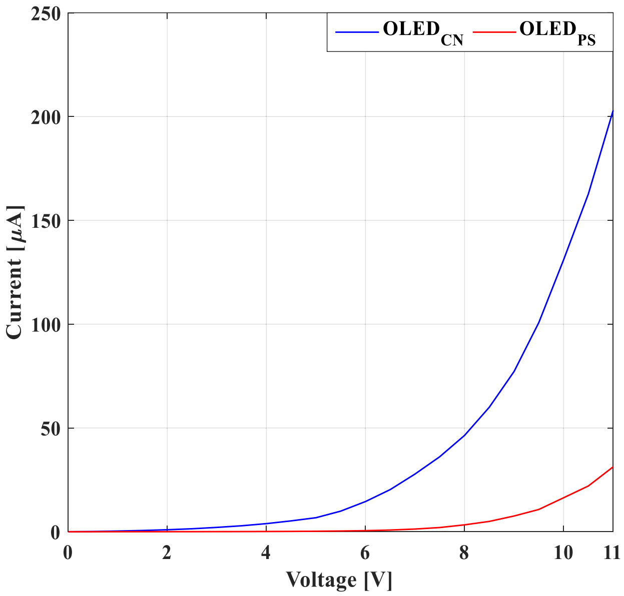

(a)

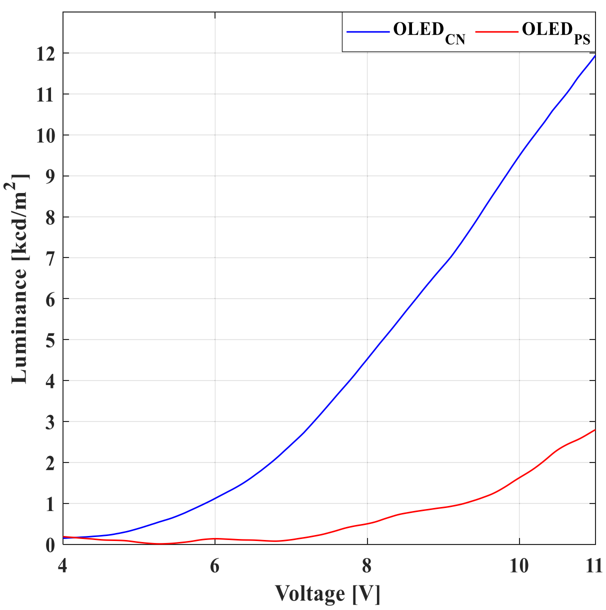

(b)

Fig. 10. (a) I–V and (b) luminance–voltage characteristics of the fabricated OLEDs using the HTLs of PEDOT:PSS (OLEDPS) and CuSCN (OLEDCN).

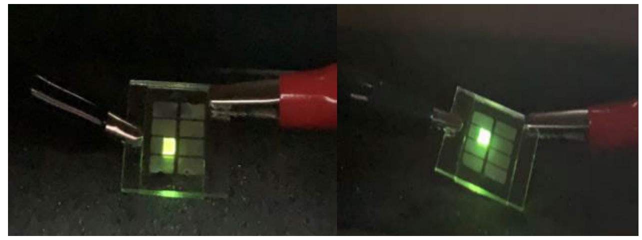

(a) (b)

Fig. 11. Photographs of fabricated OLEDs with the HTLs made of (a) PEDOT:PSS (OLEDPS) and (b) CuSCN (OLEDCN), when they were driven with the voltages of 15 and 11 V, respectively.

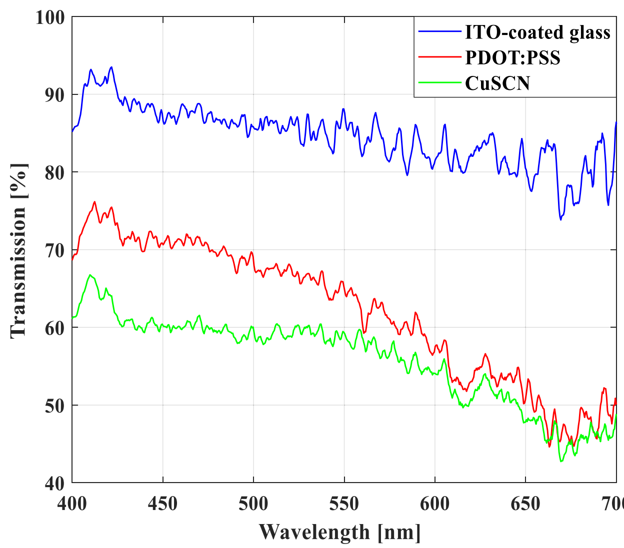

Fig. 12. Measured transmission profiles for ITO-coated glass and spin-coated PEDOT:PSS and CuSCN on its surface.

Moreover, organic materials offer more flexibility to the device than inorganic material. Therefore, full-organic LEDs are more desirable for flexible applications.

To confirm the suitability of CuSCN as HTL, the I–V and voltage–luminance curves of predried OLEDs fabricated with the HTLs of CuSCN and PEDOT:PSS are shown in Fig. 10(a) and (b), respectively. From Fig. 10(a) and (b), it can be inferred that LED$_{CN}$ can pass a higher current than their counterpart OLED$_{PS}$. At an input voltage of 11 V, the measured currents for the prototype OLEDs based on CuSCN and PEDOT:PSS layers are 202 and 32 μA, respectively. This confirms that the use of CuSCN can reduce the ohmic loss by 6.3 times at 11 V. The measured luminance in Fig. 10(b) shows that the proposed CuSCN layer as HTL increases the luminance by a factor of 4.2 from 2.8 to 12 kcd/m^2 at the same input voltage of 11 V and also significantly lowers the turn-on voltage compared to OLED$_{PS}$. To enable a fair comparison, the two OLED prototypes are compared based on their power efficiency at the heights input voltage, i.e., OLED$_{CN}$ $=$ 11 V and OLED$_{PS}$ $=$ 15 V.

The power efficiency is described as the ratio between the OLED's luminosity and power consumption [30]. In this regard, the power efficiency of OLED$_{CN}$ is 5.45E3 lm/mW, while OLED$_{PS}$ has an efficiency of 1.2E3 lm/mW. This means that deploying predried CuSCN as HTL can lead to the creation of an efficient OLED with lower power consumption and lower turn-on voltage. The photographs of these OLED prototypes, i.e., OLED$_{PS}$ and OLED$_{CN}$, operating at their highest input voltages (i.e., 15 and 11 V, respectively) are shown in Fig. 11.

So far, the advantages of using predried CuSCN as HTL to make efficient OLEDs is discussed comprehensively. To further confirm that CuSCN layer deposited by the spin coating is a transparent layer and has a relatively similar transmission profile as PEDOT:PSS, the transmission profile of deposited CuSCN and PEDOT:PSS on the ITO-coated glass was measured. To measure the transmission coefficient, a white light source was used to pass the light through the substrates, and the transmitted light was measured with the spectrometer. The

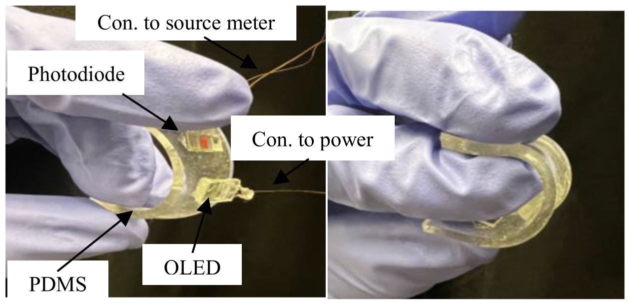

Fig. 13. (a) Photograph of the implemented flexible hybrid PPG sensor with (b) demonstration of its bendability (not used for the PPG measurement).

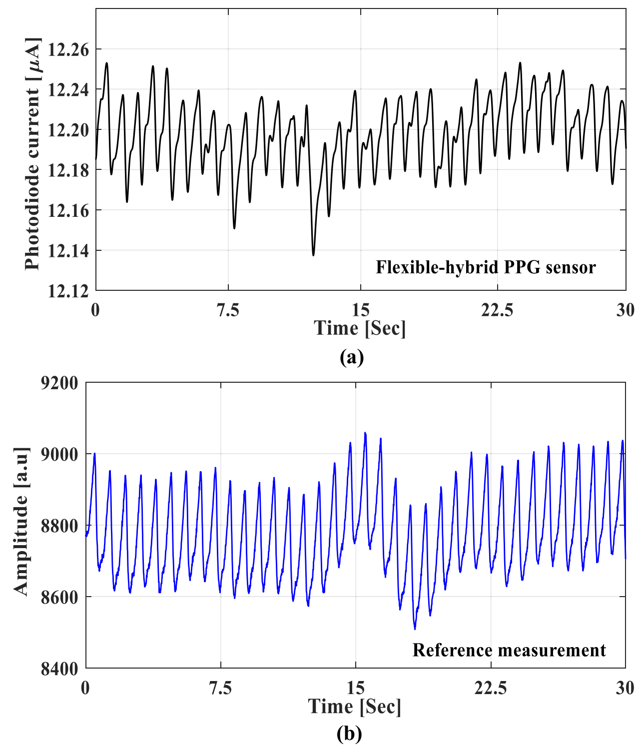

Fig. 14. PPG signals measured by (a) implemented flexible-hybrid PPG sensor and (b) commercial PPG sensor as the reference measurement.

results are shown in Fig. 12. According to this figure, at the vicinity of interested wavelength of this study (i.e., green), the ITO-coated glass with no material on its surface has a transmission coefficient of 84%, whereas the substrates with the deposited PEDOT:PSS and CuSCN exhibit the transmission of 67% and 60%, respectively, at a wavelength of 532 nm. This small difference (6%) between the transmission coefficients of PEDOT:PSS and CuSCN confirms that CuSCN has relatively similar transparency as the PEDOT:PSS layer. Therefore, it can be considered as an efficient HTL that does not block the passage of generated light.

IV. Low-Power Flexible-Hybrid PPG Sensor

To this end, it has been discussed that the OLED based on the predried HTL of CuSCN is more efficient than an OLED fabricated with the HTL of PEDOT:PSS. To further confirm that the highly efficient $OLED_{CN}$ proposed in this study was a viable solution for low-power PPG sensing systems, it was molded into a flexible substrate, i.e., polydimethylsiloxane (PDMS), after being diced. A commercially available photodetector from Osram (model SFH 7072) capable to measure PPG signals was placed near $OLED_{CN}$ to construct a flexible hybrid PPG sensor. The bending capability of the implemented PPG sensing system with the fabricated $OLED_{CN}$ when integrated with the photodetector on a flexible substrate is demonstrated in Fig. 13. It is worth mentioning that for the measuring PPG signals depicted in Fig. 14, the flexible PPG sensor was placed on a desk (without any bending) and the left index finger of the volunteer was placed on the fabricated $OLED_{CN}$ and the photodetector of the PPG sensor. The $OLED_{CN}$ and photodiode were placed relatively close to each other on the flexible substrate (PDMS) to acquire PPG signal in reflectance mode.

To verify the accuracy of the PPG signals acquired by the implemented flexible-hybrid PPG sensor, a commercial PPG sensor from Maxim integrated (MAX30101EFD+) was used as a reference measurement on the right index finger. We chose such a commercially available sensor because, first, the driving current of LEDs can be controlled, second, it has a high accuracy that is relatively close to FDA-approved pulse oximetries [31], and third, it has an efficient postsignal processing algorithm. The PPG signal collection experiment was in accordance with the Deceleration of Helsinki and was approved by the Institutional Review Board of McGill University (study number: A04-M21-19B, approval date: 17 April 2019). To capture PPG signals with high quality, the driving current of the reference sensor was needed to be set to 10.5 mA, while the proposed $OLED_{CN}$ driving current was set to 0.2 mA. The PPG signals was measured from the implemented flexible-hybrid system by directly measuring the photodiode current with the source meter without applying any signal processing techniques or implementing any circuit conditioning. PPG signals measured by the flexible-hybrid sensor and the reference one for a duration of 30 s while the subject was in the rest position are shown in Fig. 14. It is worth mentioning that the output signal of the reference measurement is a converted analog to digital signal with an arbitrary unit (a.u.), in contrast, the output signal of the flexible hybrid PPG sensor implemented by us is an analog current with a unit of μA. It can be seen that the signal measured by our flexible-hybrid system has a relatively similar morphology (i.e., frequency and number of detectable peaks) as the PPG signal measured by the reference sensor. In PPG signal, the number of peaks is an indicator of HR. Consequently, the estimated HR from the PPG signal measured by the flexible hybrid monitoring system we developed is 70 bpm, and the reference measurement shows an HR of 72. Such a comparative value for the estimated HR proves that the low-power OLED proposed in this study can be integrated into a flexible system for effective and efficient cardiac activities estimation.

To further confirm the competence of the proposed predried $OLED_{CN}$ as a relatively low-power solution for PPG singing system, its performance was compared to the state of the art as well as commercially available LED utilized for PPG

TABLE I
PERFORMANCE COMPARISON BETWEEN THE REPORTED LEDS IN THE LITERATURE AND $OLED_{CN}$ PROPOSED IN THIS STUDY FOR PPG SENSING

Parameter \ Ref.	[32]	[33]	[25]	[34]	[24]	**This work**
Wavelength [nm]	532	532	520	523	530	**532**
Type	organic	organic	organic	solid-state	Organic	**Organic**
Supply voltage [V]	10	10	5	4.1	3.3	**11**
LED Driving current [mA]	16	0.4	0.96	20	0.390	**0.202**
Power consumption [mW]	160	4	4.8	82	1.28	**2.2**
Luminance [ca/m^2]	136,986	10,000	1,000	0.9*	6,222	**12,000**
Power efficiency [lm/mW]	8.5E2	2.5E3	2.08E2	1E-2*	1.72E2	**5.45E3**

*Estimated

measurements, as shown in Table I. One fact is obvious that OLED with the lowest driving current belongs to one reported in this study. It can be seen that the proposed $OLED_{CN}$ has the highest power efficiency, since it could generate high luminance at a low input electrical power. It is worth mentioning that the OLED proposed in the recently published study [24] also requires a low operating current. However, it should not be ignored that such an OLED has a very low luminance. Therefore, the authors had to use it in the form of an array (i.e., two OLEDs) for precise measurement of PPG signals.

V. CONCLUSION

In this work, a novel fabrication step, namely, predrying, is proposed to improve the performance of OLEDs. The predrying method with the capability of employing in solution-based fabrication processes allows the solution to dwell on the substrate for a certain short time before the spin coater is turned on. It is experimentally shown that the predrying step for OLEDs using the HTL of PEDOT:PSS can reduce the ohmic loss by a factor of 2.41, in addition to reducing the turn-on voltage by 0.9 V and increasing the luminance by a factor 1.3 from 5.2 to 6.8 kcd/m^2 at 15 V. Advantageously, this performance improvement has almost no effect on the emission spectrum (i.e., peak emission wavelength), when compared to the OLED fabricated without predrying step. To further improve the competence of OLED, the use of CuSCN as an efficient HTL instead of the conventional PEDOT:PSS was proposed. The prototype OLEDs based on the predried HTL of CuSCN exhibited a luminance of 12 kcd/m^2 at a voltage of 11 V. Through holistic performance comparison, it was found that the fabricated OLEDs with the predried HTLs made of CuSCN and PEDOT:PSS had power efficiencies of 5.45E3 and 1.2E3 lm/mW, at 11 and 15 V, respectively.

Due to the superior performance of the proposed OLED based on the predried HTL of CuSCN, its behavior as a light source for PPG sensing systems was surveyed. In this article, the OLED was implemented in the form of a flexible-hybrid sensor system, in which the OLED and a commercial photodiode are housed in a flexible substrate. It was demonstrated that our implemented flexible-hybrid PPG sensor can capture a high-quality PPG signal with relatively low power consumption compared to a commercial PPG sensor. Finally, the competency of the proposed OLED with the predried HTL of CuSCN as a low-power solution for PPG sensor technology was highlighted by comparing its performance with the state of the art.

REFERENCES

[1] Y. Zhuang et al., "A survey of positioning systems using visible LED lights," *IEEE Commun. Surveys Tuts.*, vol. 20, no. 3, pp. 1963–1988, 3rd Quart., 2018.

[2] F.-C. Wang, C.-W. Tang, and B.-J. Huang, "Multivariable robust control for a red–green–blue LED lighting system," *IEEE Trans. Power Electron.*, vol. 25, no. 2, pp. 417–428, Feb. 2010.

[3] L. Teixeira, F. Loose, J. M. Alonso, C. H. Barriquello, V. A. Reguera, and M. A. Dalla Costa, "A review of visible light communication LED drivers," *IEEE J. Emerg. Sel. Top. Power Electron.*, vol. 10, no. 1, pp. 919–933, Feb. 2021.

[4] J. Allen, "Photoplethysmography and its application in clinical physiological measurement," *Physiological Meas.*, vol. 28, no. 3, pp. R1–R39, Mar. 2007.

[5] S. Nabavi and S. Bhadra, "A robust fusion method for motion artifacts reduction in photoplethysmography signal," *IEEE Trans. Instrum. Meas.*, vol. 69, no. 12, pp. 9599–9608, Dec. 2020.

[6] S. Nabavi and S. Bhadra, "Smart mandibular advancement device for intraoral monitoring of cardiorespiratory parameters and sleeping postures," *IEEE Trans. Biomed. Circuits Syst.*, vol. 15, no. 2, pp. 248–258, Apr. 2021.

[7] C.-K. Li and Y.-R. Wu, "Study on the current spreading effect and light extraction enhancement of vertical GaN/InGaN LEDs," *IEEE Trans. Electron Devices*, vol. 59, no. 2, pp. 400–407, Feb. 2012.

[8] S. Nabavi and S. Bhadra, "Flexible inductive wireless power transfer system with an onboard temperature sensor," in *Proc. IEEE Int. Conf. Flexible Printable Sensors Syst. (FLEPS)*, Jun. 2021, pp. 1–4.

[9] S. Nabavi, S. Debbarma, and S. Bhadra, "A smart mandibular advancement device for intraoral cardiorespiratory monitoring," in *Proc. 42nd Annu. Int. Conf. IEEE Eng. Med. Biol. Soc. (EMBC)*, Jul. 2020, pp. 4079–4084.

[10] S. Nabavi, Y. Chen, N. Lasry, and S. Bhadra, "Fully flexible organic LED fabricated by a solution-based process," in *Proc. IEEE Int. Conf. Flexible Printable Sensors Syst. (FLEPS)*, Jul. 2022, pp. 1–4.

[11] A. Salehi, X. Fu, D. Shin, and F. So, "Recent advances in OLED optical design," *Adv. Funct. Mater.*, vol. 29, no. 15, Apr. 2019, Art. no. 1808803.

[12] C. W. Tang and S. A. VanSlyke, "Organic electroluminescent diodes," *Appl. Phys. Lett.*, vol. 51, no. 12, pp. 913–915, 1987.

[13] G. Gustafsson, Y. Cao, G. M. Treacy, F. Klavetter, N. Colaneri, and A. J. Heeger, "Flexible light-emitting diodes made from soluble conducting polymers," *Nature*, vol. 357, no. 6378, pp. 477–479, Jun. 1992.

[14] M. A. Baldo, D. F. O'Brien, M. E. Thompson, and S. R. Forrest, "Excitonic singlet-triplet ratio in a semiconducting organic thin film," *Phys. Rev. B, Condens. Matter*, vol. 60, no. 20, pp. 14422–14428, Nov. 1999.

[15] T. P. Nguyen, P. Le Rendu, N. N. Dinh, M. Fourmigué, and C. Mézière, "Thermal and chemical treatment of ITO substrates for improvement of OLED performance," *Synth. Met.*, vol. 138, nos. 1–2, pp. 229–232, Jun. 2003.

[16] M. Yahya and M. R. Fadavieslam, "The effects of argon plasma treatment on ITO properties and the performance of OLED devices," *Opt. Mater.*, vol. 120, Oct. 2021, Art. no. 111400.

[17] Y. H. Huh, O. E. Kwon, and B. Park, "Triple-stacked hole-selective layers for efficient solution-processable organic semiconducting devices," *Opt. Exp.*, vol. 23, no. 11, p. A625, 2015.

[18] Z. Chen, Z. Deng, D. Xu, C. Liang, X. Li, and K. Zhao, "High performance organic light-emitting diodes (OLEDs) with molybdenum oxide (MoOx) as the buffer layer," in *Proc. Organic Mater. Devices Displays Energy Convers.*, 2007, p. OTuD3.

[19] M. Kim, C. Lim, D. Jeong, H.-S. Nam, J. Kim, and J. Lee, "Design of a MoO_x/Au/MoO_x transparent electrode for high-performance OLEDs," *Org. Electron.*, vol. 36, pp. 61–67, Sep. 2016.

[20] A. Turak, "On the role of LiF in organic optoelectronics," *Electron. Mater.*, vol. 2, no. 2, pp. 198–221, Jun. 2021.

[21] Y. Wang et al., "Green to white to blue OLEDs by using PBD as a chromaticity-tuning layer," *Displays*, vol. 25, no. 5, pp. 237–239, Dec. 2004.

[22] Z. Wang et al., "Energy level engineering of PEDOT: PSS by antimonene quantum sheet doping for highly efficient OLEDs," *J. Mater. Chem. C*, vol. 8, no. 5, pp. 1796–1802, 2020.

[23] Y.-Q. Zheng et al., "Highly efficient red fluorescent organic light-emitting diodes by sorbitol-doped PEDOT: PSS," *J. Phys. D, Appl. Phys.*, vol. 51, no. 22, 2018, Art. no. 225302.

[24] R. K. Pandey and P. C.-P. Chao, "A dual-channel PPG readout system with motion-tolerant adaptability for OLED-OPD sensors," *IEEE Trans. Biomed. Circuits Syst.*, vol. 16, no. 1, pp. 36–51, Feb. 2022.

[25] Y. Lee et al., "Sticker-type hybrid photoplethysmogram monitoring system integrating CMOS IC with organic optical sensors," *IEEE J. Emerg. Sel. Topics Circuits Syst.*, vol. 7, no. 1, pp. 50–59, Mar. 2017.

[26] A. Dualeh, N. Tétreault, T. Moehl, P. Gao, M. K. Nazeeruddin, and M. Grätzel, "Effect of annealing temperature on film morphology of organic–inorganic hybrid pervoskite solid-state solar cells," *Adv. Funct. Mater.*, vol. 24, no. 21, pp. 3250–3258, Jun. 2014.

[27] B. Friedel et al., "Effects of layer thickness and annealing of PEDOT: PSS layers in organic photodetectors," *Macromolecules*, vol. 42, no. 17, pp. 6741–6747, Sep. 2009.

[28] X. Guo et al., "Highly efficient perovskite solar cells based on a dopant-free conjugated DPP polymer hole transport layer: Influence of solvent vapor annealing," *Sustain. Energy Fuels*, vol. 2, no. 10, pp. 2154–2159, 2018.

[29] M. Cinquino et al., "Effect of surface tension and drying time on inkjet-printed PEDOT: PSS for ITO-free OLED devices," *J. Science, Adv. Mater. Devices*, vol. 7, no. 1, Mar. 2022, Art. no. 100394.

[30] S. Yadav, P. Mittal, and S. Negi, "Recent advancements over a decade for organic light-emitting diodes: From structural diversity, role of layers, colour emission, material classification, performance improvement, fabrication to applications," *Bull. Mater. Sci.*, vol. 45, no. 3, pp. 1–26, Jun. 2022.

[31] S. H. Browne et al., "Smartphone biosensor with app meets FDA/ISO standards for clinical pulse oximetry and can be reliably used by a wide range of patients," *Chest*, vol. 159, no. 2, pp. 724–732, Feb. 2020.

[32] C. M. Lochner, Y. Khan, A. Pierre, and A. C. Arias, "All-organic optoelectronic sensor for pulse oximetry," *Nature Commun.*, vol. 5, no. 1, pp. 1–7, Dec. 2014.

[33] T. Yokota et al., "Ultraflexible organic photonic skin," *Sci. Adv.*, vol. 2, no. 4, Apr. 2016, Art. no. e1501856.

[34] *OSRAM*. Accessed: Oct. 14, 2022. [Online]. Available: https://ams-osram.com/products

Seyedfakhreddin (Koorosh) Nabavi (Member, IEEE) was born in Hamedan, Iran, in 1991. He received the B.Sc. degree (Hons.) in biomedical engineering (bioelectric) from the Sahand University of Technology, Tabriz, Iran, in 2013, the M.Sc. degree in electrical and electronic engineering from Ozyegin University, Istanbul, Turkey, in 2015, and the Ph.D. degree from the Memorial University of Newfoundland, St. John's, NL, Canada, in April 2019.

He was a Post-Doctoral Fellow with the Department of Electrical and Computer Engineering, McGill University, Montreal, QC, Canada. He is currently a Research Associate with the École de Technologie Supérieure, Montreal, a constituent of the University of Quebec, Quebec, QC, Canada. He has authored or coauthored over 38 publications and holds eight pending patents applications in the areas of sensors and wearable devices. His current research interests include the design and modeling of MEMS transducers and actuators for industrial and biomedical applications and the design of analog circuits, such as sensor interfaces and power management systems.

Dr. Nabavi was identified as a Top Reviewer for *Applied Physics Letters* (APL) in 2018.

Hossein Anabestani is currently pursuing the Ph.D. degree with the Department of Electrical and Computer Engineering, McGill University, Montreal, QC, Canada.

His research work at McGill University focuses on the development of solution-processed organic photoplethysmography (PPG) sensors and the estimation of cardiorespiratory parameters from PPG signals. His current research interests include printed and flexible sensors, wearable technology, and optoelectronics.

Sharmistha Bhadra (Member, IEEE) is currently an Assistant Professor with the Department of Electrical and Computer Engineering, McGill University, Montreal, QC, Canada. Her research program at McGill University leverages conventional design and development tools as well as flexible printed electronics technology to find cost effective and high-performance innovative electronic technology. She has authored or coauthored over 78 articles and one book chapter and holds four patents in sensors and wearables area. Her current research interests include area of printed and flexible hybrid electronics, microelectronics, microelectromechanical systems, and sensors and wearables.